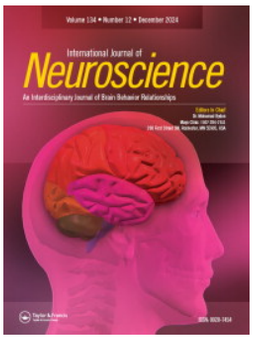

International Journal of Neuroscience

ISSN: (Print) (Online) Journal homepage: www.tandfonline.com/journals/ines20

"Grade 4 Astrocytoma vs Grade 4 Glioblastoma: Is there any clue in H&E?"

Cevriye Cansiz Ersöz, Havva Berber & Aylin Heper

To cite this article: Cevriye Cansiz Ersöz, Havva Berber & Aylin Heper (16 Dec 2024): "Grade 4 Astrocytoma vs Grade 4 Glioblastoma: Is there any clue in H&E?", International Journal of Neuroscience, DOI: 10.1080/00207454.2024.2441994

To link to this article: https://doi.org/10.1080/00207454.2024.2441994

"Grade 4 Astrocytoma vs Grade 4 Glioblastoma: Is there any clue in H&E?"

Cevriye Cansiz Ersöz*, MD, Havva BERBER, MD, Aylin HEPER, MD, Prof.

Department of Pathology, Ankara University Medical School

***Corresponding author:** Cevriye Cansiz Ersöz, Ankara University Faculty of Medicine, Department of Pathology, 06100, Sihhiye, Ankara, Turkey. cevriye80@yahoo.com

Abstract:

Gliomas are the most common primary tumors of the central nervous system. The fifth edition of the World Health Organization (WHO) Classification of Tumors of the CNS identifies IDH mutant astrocytomas grade 4 and IDH wild type glioblastomas grade 4 as distinct entities. This study aimed to identify morphological indicators that could predict IDH mutation status in grade 4 diffuse astrocytomas and grade 4 glioblastomas among fifty patients from two groups. Hematoxylin and eosin (H&E)-stained tumor slides were scanned using a digital scanner and further histopathological examinations were performed on digital images, with additional calculations and measurements. The study showed that, IDH-wildtype glioblastomas and IDH-mutant grade 4 astrocytomas exhibit unique morphological features, particularly in relation to levels of necrosis, microvessel density, and the presence of "C" or "Ring" shape giant cells. Despite advancements in genomic biomarker technology, histology remains an essential tool for predicting patient outcomes. Therefore, pathologists must continue to investigate and document the morphological implications of molecular changes in CNS tumors.

Keywords: Gliomas, Glioblastoma, Astrocytoma, Grade 4, Morphology

Introduction:

Gliomas are adults' most frequent central nervous system (CNS) primary tumors. Although there are significant progress in defining their biology in recent years, they still remain uncurable. An integrated diagnosis based on histological features and molecular markers is crucial for the accurate classification of adult diffuse gliomas, according to the fifth edition of the World Health Organization (WHO) Classification of Tumors of the CNS [1].

Mutations in the isocitrate dehydrogenase (IDH) gene are recognized as early genetic events in the development of gliomas. These mutations modify IDH enzymes, resulting in the generation of the oncometabolite 2-hydroxyglutarate, which inhibits DNA demethylation and promotes genome-wide DNA hypermethylation. [1, 2]. This molecular alteration carries profound implications for diagnosis, treatment, and prognosis. In particular, IDH mutations are generally linked to improved outcomes in high-grade gliomas, setting IDH-mutant (IDHmut) tumors apart as biologically distinct from IDH-wildtype (IDHwt) tumors. While they may exhibit similar histomorphological characteristics, such as palisading necrosis and microvascular proliferation, grade 4 astrocytomas and glioblastomas exhibit marked biological differences. Therefore, evaluating IDH mutation status in gliomas is critical.

The majority of IDH mutations are missense mutations in the IDH1 gene at codon 132, leading to an arginine-to-histidine substitution (R132H), which can be identified using mutation-specific immunohistochemistry (IHC) [1, 2]. Recent WHO guidelines advocate for IDH mutation analysis in instances where immunohistochemistry results are negative. However, achieving an integrated diagnosis that includes both histological and molecular characteristics is often time-consuming, labor-intensive, and expensive. Therefore, identifying morphological clues predictive of IDH mutation status could provide a more efficient diagnostic pathway. **Furthermore, when the world was considered as a whole; in non-developed countries it is evident that in resource-limited settings where molecular diagnostics may not be readily available, morphologic clues are much more important to accurate diagnosis.**

In recent years, whole-slide imaging (WSI) obtained by digital scanners has become increasingly prevalent in pathology practice [3, 4]. Additionally, artificial intelligence (AI) programs that leverage deep learning have shown promise in automating histopathological diagnoses across a range of diseases, including gliomas [5-7]. These technologies hold the potential to enhance both the efficiency and accuracy of diagnostic processes for pathologists. However, for these tools to attain widespread clinical applicability, the morphological features that distinguish different tumor types must be clearly defined and integrated into AI algorithms.

Recent research in gliomas utilizing digital pathology has predominantly concentrated on tumor grading, relying on four essential morphological criteria traditionally employed by pathologists: nuclear atypia, mitotic activity, endothelial proliferation, and necrosis [6, 8-12]. Additionally, other studies have demonstrated that deep learning models can forecast IDH mutation status and prognosis by integrating morphological features from whole slide images with demographic and clinical data [13-15].

In this study, we aimed to identify morphological clues predictive of IDH mutation status in grade 4 diffuse astrocytomas and grade 4 glioblastomas, using a cohort of patients matched for age, sex, and tumor localization.

Materials and Methods:

Study Cohorts:

Due to its relatively rare occurrence, approximately 27 cases of IDH-mutant grade 4 astrocytoma were found in the archive which diagnosed between 2016 and 2023 in our department. Two of these were not included in the study because they did not have optimal section and stain quality, and the study was planned with the remaining 25 cases. These cases exhibited classic histological features, such as palisading necrosis and microvascular proliferation. Age, sex, and tumor localization were recorded. **To avoid any clinicopathological bias, each IDHmut case matched with an identical IDHwt patient of the same age, gender, and location by scanning the archive of 362 patients diagnosed during the same period.**

Imaging Analysis:

Fifty hematoxylin and eosin (H&E)-stained tumor slides were scanned using a digital scanner (3D Histech Pannoramic 250 Flash3) and analyzed using Case Viewer software. Further histopathological examinations were performed on digital images, with additional calculations and measurements obtained using the Quant Center Application.

Tumor nuclei were manually identified individually, and cellularity was assessed by counting cells per square millimeter in software-selected tumor "hot spots" (Figure 1). Also all vascular lumens were manually identified one-by-one and, microvessel density was evaluated by scanning hot spots and counting vascular lumens per square millimeter. Necrotic areas were manually annotated, and the percentage of necrosis was calculated relative to the total tumor area. The presence of "ring" or "C"-shaped nuclei, resulting from nuclear segmentation and peripheral location; and the major axis length of tumor giant cells were also recorded. Inflammatory cells were categorized as absent (0), present (1+), or abundant (2+). Mitotic activity was evaluated by counting mitotic figures in 10 high-power fields (HPFs), representing 2 mm^2 of tumor tissue.

Statistical Analyses:

Statistical analysis was performed using the chi-squared test for frequency comparisons and the Mann-Whitney U test for continuous variables. A p-value <0.05 was considered statistically significant.

Ethics Statement:

Institutional Review Board (IRB) approval was obtained for this study (approval code 2024/16, date 05 September 2024). No additional tissue sectioning, staining, or testing was performed on patient samples.

Results:

Although IDHwt tumors exhibited slightly higher cellularity than IDHmut tumors, no statistically significant difference was observed between groups (IDHwt: 6831.29 cells/mm²; IDHmut: 6349.45 cells/mm²; $p>0.05$). Necrosis was present in 96% of IDHmut cases (24/25) and in all IDHwt cases (25/25). Microvascular proliferation was observed in all tumors. The extent of necrosis was significantly higher in IDHwt tumors compared to IDHmut tumors (42.24% vs. 22.29%; $p=0.004$). Microvessel density was also significantly higher in IDHwt tumors (14.88/mm² vs. 8.40/mm²; $p<0.001$). Mitotic activity was significantly greater in the IDHwt group (10.84/10 HPF) compared to the IDHmut group (8.12/10 HPF; $p=0.033$). No statistically significant difference was observed in the major axis length of tumor giant cells between the two groups (IDHmut: 36.8 µm vs. IDHwt: 37.1 µm; $p>0.05$). Segmented, "ring" or "C"-shaped nuclei were identified in 84% of IDHmut cases (21/25) and only 8% of IDHwt cases (2/25), a difference that was statistically significant ($p<0.001$) (Figure 2 and 3). Inflammatory cells were present in all tumors, with no significant difference in their abundance between the two groups ($p>0.05$). A summary of all findings is provided in Table 1 and demonstrated in Graphic 1.

Discussion:

The 2021 update to the WHO Classification of CNS Tumors recognizes IDH-mutant astrocytoma grade 4 and IDH-wildtype glioblastoma grade 4 as separate entities. The IDH mutation status plays a critical role in clinical treatment planning, making it imperative to differentiate between these tumors. While ascertaining IDH mutation status can be complex, morphological differences may provide a means of distinction. Our study reveals that IDH-wildtype glioblastomas and IDH-mutant grade 4 astrocytomas display unique morphologic characteristics, particularly concerning the levels of necrosis, microvessel density, and the presence of “C” or “Ring” shape giant cells.

Tumor necrosis is a well-known indicator of aggressiveness and prognosis across various tumor types and has long been used in grading glial tumors [1]. Recent studies using whole slide imaging (WSI) have proven necrosis to be a reliable parameter for grading gliomas [8–12]. Additionally, some studies suggest that machine learning may predict IDH mutation status based on WSI analysis [14, 15]. While models trained on grade 2 to grade 4 cases can effectively distinguish high-risk from low-risk patients, their ability to differentiate within the same grade remains limited. In our study, the extent of necrosis was significantly greater in the IDH-wildtype group compared to the IDH-mutant group ($p = 0.004$), consistent with the aggressive nature of glioblastomas.

Angiogenesis and tumor vasculature are critical factors in tumor progression. To further investigate vascular differences between these two high-grade astrocytomas, we analyzed microvessel density. Previous studies have shown that IDH-wildtype tumors exhibit stronger vascular processes during progression, as observed at the transcriptomic level [16]. The increased vascular supply in IDH-wildtype tumors is associated with more rapid progression. Consistent with these findings, our study demonstrated significantly higher microvessel density in the IDH-wildtype group compared to the IDH-mutant group.

Multinucleated giant cells can appear in varying proportions in grade 4 glial tumors. According to the most recent WHO update, giant cell glioblastoma should only be diagnosed when giant cells are the predominant histopathologic component [1, 2]. In our cohort, none of the tumors, either in the IDH-mutant or IDH-wildtype groups, contained giant cells as a dominant feature. Although no significant difference was observed in the length or nuclear segmentation of giant cells, an increased nucleocytoplasmic ratio was noted in the IDH-wildtype group. In contrast, in the IDH-mutant group, we observed "C"- or "ring"-shaped nuclei due to the peripheral nuclear location ($p < 0.001$). While recent studies have identified specific morphological features that differentiate oligodendrogliomas from astrocytomas, such as greater circularity and less eccentricity in oligodendroglioma cells [17], no conclusive data define the morphological impact of IDH mutation status.

Finally, as detected in previous AI-based morphometric analyses, determining IDH mutation status in tumors of different grades, which have very different patterns, is quite successful and seems promising for the future. However, in addition to morphological patterns, by incorporating data at a more micromorphometric level, i.e., on a cell-by-cell basis and nuclear localization basis, it will be possible to estimate the IDH status in tumors of the same grade and pattern.

Conclusion

Despite advances in genomic biomarker technology, histology remains a crucial tool for predicting patient outcomes. The phenotypic information provided by histologic analysis reflects the cumulative effect of molecular changes on tumor cell behavior and serves as a visual marker of disease aggressiveness. Therefore, pathologists should continue to explore and document the morphologic effects of molecular alterations in CNS tumors.

Limitations

This study has several limitations, including a small patient cohort and the exclusion of cases with recurrence or progression because of the fact that morphological effects secondary to the first operation. In recurrent tumors the extent of necrosis and the reparative changes may affect the appearance of vascular proliferation. These findings should be validated in larger, more diverse patient populations.

References:

1. Louis DN, P.A., Wesseling P, et al. , The 2021 WHO classification of tumors of the central nervous system: a summary. Neuro Oncol., 2021. **8**(23): p. 1231–1251.
2. Komori, T., Grading of adult diffuse gliomas according to the 2021 WHO Classification of Tumors of the Central Nervous System. Laboratory Investigation 2022. **102**: p. 126-133.
3. Farris, A.B., et al., Whole Slide Imaging for Analytical Anatomic Pathology and Telepathology: Practical Applications Today, Promises, and Perils. Arch Pathol Lab Med, 2017. **141**(4): p. 542-550.
4. Mobadersany, P., et al., Predicting cancer outcomes from histology and genomics using convolutional networks. Proc Natl Acad Sci U S A, 2018. **115**(13): p. E2970-E2979.
5. Kong, J., et al., Machine-based morphologic analysis of glioblastoma using whole-slide pathology images uncovers clinically relevant molecular correlates. PLoS One, 2013. **8**(11): p. e81049.
6. Jin, L., et al., A multi-center performance assessment for automated histopathological classification and grading of glioma using whole slide images. iScience, 2023. **26**(11): p. 108041.
7. Asami Yonekura, H.K., V. B. Surya Prasath, Bruce J. Aronow, Haruhiko Takase, Automatic disease stage classification of glioblastoma multiforme histopathological images using deep convolutional neural network. Biomedical Engineering Letters (2018) 8:321–327, 2018. **8**: p. 321-327.
8. Rathore, S., et al., Glioma Grading via Analysis of Digital Pathology Images Using Machine Learning. Cancers (Basel), 2020. **12**(3).
9. Jose, L., et al., Artificial Intelligence-Assisted Classification of Gliomas Using Whole Slide Images. Arch Pathol Lab Med, 2023. **147**(8): p. 916-924.
10. Su, F., et al., Annotation-free glioma grading from pathological images using ensemble deep learning. Heliyon, 2023. **9**(3): p. e14654.
11. Wang, W., et al., Neuropathologist-level integrated classification of adult-type diffuse gliomas using deep learning from whole-slide pathological images. Nat Commun, 2023. **14**(1): p. 6359.
12. Despotovic, V., et al., Glioma subtype classification from histopathological images using in-domain and out-of-domain transfer learning: An experimental study. Heliyon, 2024. **10**(5): p. e27515.
13. Jiang, S., G.J. Zanazzi, and S. Hassanpour, Predicting prognosis and IDH mutation status for patients with lower-grade gliomas using whole slide images. Sci Rep, 2021. **11**(1): p. 16849.
14. Liechty, B., et al., Machine learning can aid in prediction of IDH mutation from H&E-stained histology slides in infiltrating gliomas. Sci Rep, 2022. **12**(1): p. 22623.
15. Nakagaki, R., et al., Deep learning-based IDH1 gene mutation prediction using histopathological imaging and clinical data. Comput Biol Med, 2024. **179**: p. 108902.
16. Alvarez-Torres, M.D.M., et al., Vascular differences between IDH-wildtype glioblastoma and astrocytoma IDH-mutant grade 4 at imaging and transcriptomic levels. NMR Biomed, 2023. **36**(11): p. e5004.
17. Meenakshi Gupta, A.D., Daniel J. Brat, Clarifying the diffuse gliomas: an update on the morphologic features and markers that discriminate oligodendroglioma from astrocytoma. American Journal of Clinical Pathology, 2005. **124**(5): p. 755-768.

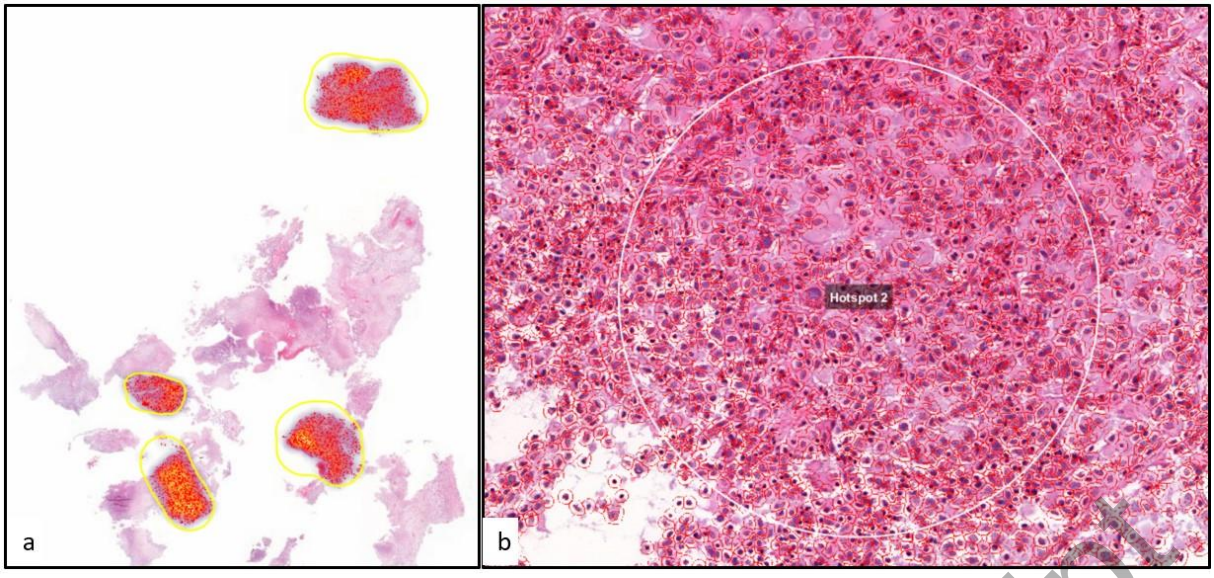

Figure 1: a & b. Cellularity counting in "hot spots"

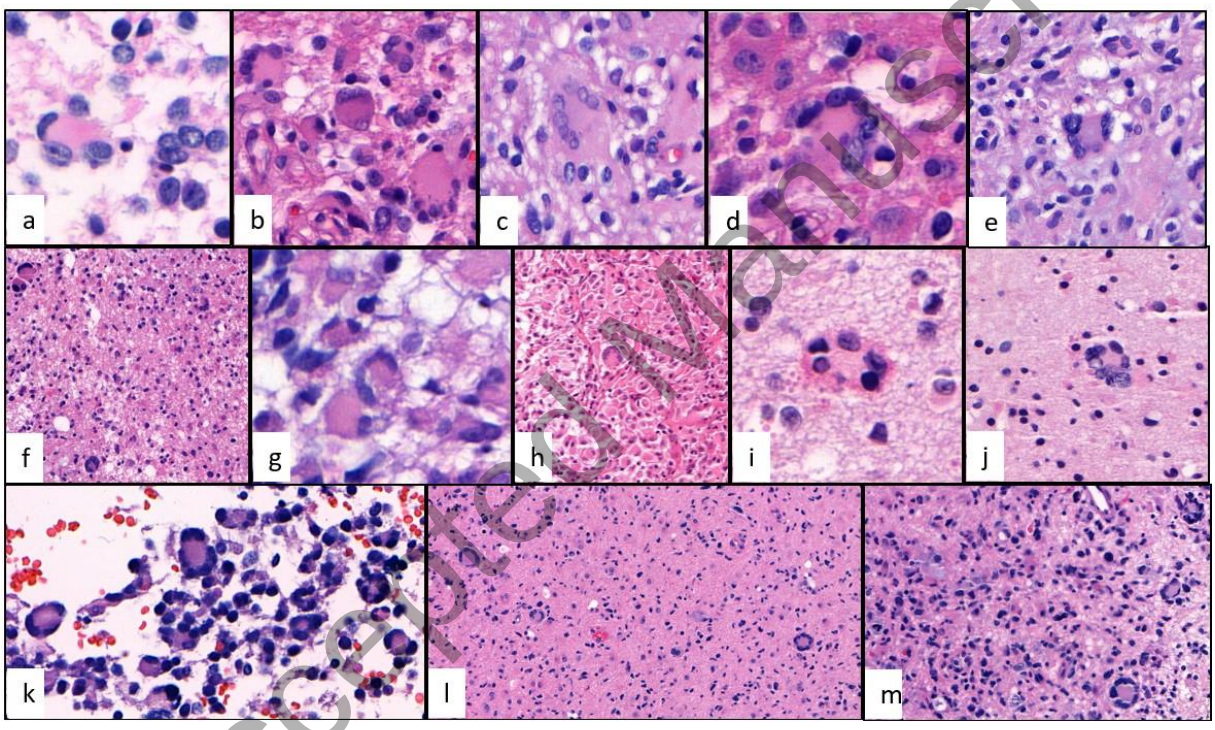

Figure 2: 2a-2m. Tumor giant cells with segmented nucleus with peripherally located that cause “C” or “Ring” shape in IDHmut tumors (H&E staining with x100 between x400)

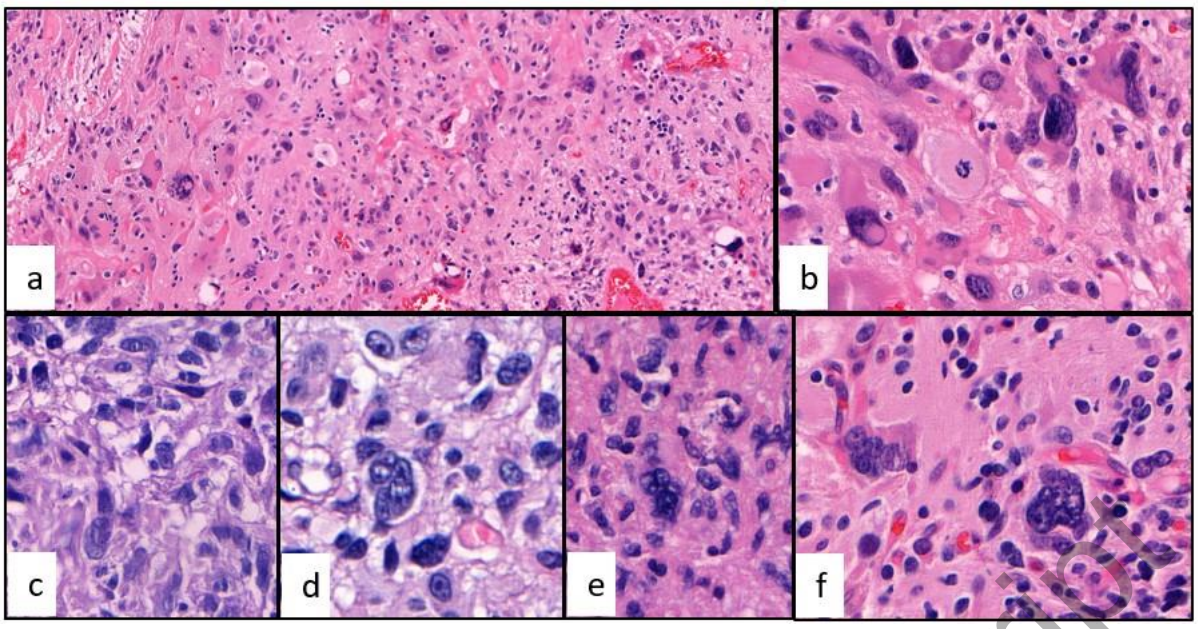

Figure 3: 3a- 3f. Tumor giant cells in IDHwt tumour. They have high nucleocytoplasmic ratio, and with multinucleated not peripherally location (H&E staining with x100 between x400)

Graphic 1: Graphical representation of statistically significant findings

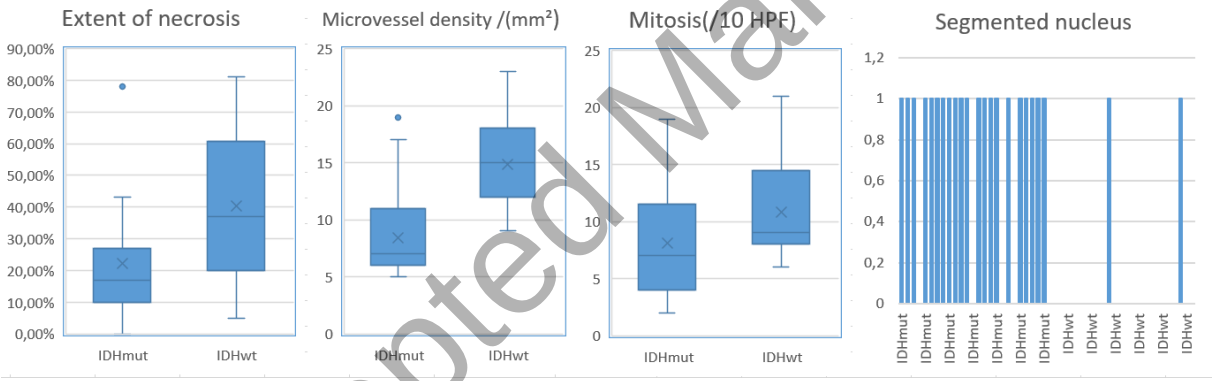

Table 1: Summary of morphologic differences between two groups.

	Cellularity	**Necrosis**	**Extent of necrosis**	**Microvessel density**	**Mitosis (/10 HPF)**	**Major axis lenght**	**Segmented nucleus**	**İnflammatory cells**
IDHwt (n:25)	6831.29 cells/mm²	25/25	42.24%	14.88/mm²	10.84	37.1 µm	8% (2/25)	25/25
IDHmut (n:25)	6349.45 cells/mm²	24/25	22.29%	8.40/mm²	8.12	36.8 µm	84% (21/25)	25/25
p value	p>0.05	p>0.05	**p=0.004**	**p<0.001**	**p=0.033**	p>0.05	**p<0.001**	p>0.05